ELSEVIER

Journal of Alloys and Compounds 330–332 (2002) 400–403

Journal of ALLOYS AND COMPOUNDS

www.elsevier.com/locate/jallcom

Analysis of the fracture behavior of a hydrided cladding tube at elevated temperatures by fracture mechanics

Shinsuke Yamanaka[a], Masatoshi Kuroda[a,*], Daigo Setoyama[a], Masayoshi Uno[a], Kiyoko Takeda[b], Hiroyuki Anada[b], Fumihisa Nagase[c], Hiroshi Uetsuka[c]

[a]*Department of Nuclear Engineering, Graduate School of Engineering, Osaka University, Yamadaoka 2-1, Suita, Osaka 565-0871, Japan*
[b]*Sumitomo Metal Industries, Ltd., Fuso-cho, Amagasaki, Hyogo-ken 660-0891, Japan*
[c]*Department of Reactor Safety Research, Japan Atomic Energy Research Institute, Tokai-mura, Ibaraki-ken 319-1195, Japan*

Abstract

An analysis, based on fracture mechanics at elevated temperatures, has been carried out for several types of hydrided Zircaloy cladding tubes to elucidate the fracture behavior of high burn up light water reactor fuel cladding during reactivity initiated accidents. Fracture mechanics parameters such as stress intensity factor, *J*-integral and plastic yield load were estimated by a finite element method analysis, and the material properties of α-phase of zirconium required for the analysis were obtained by tensile tests at elevated temperatures. The failure assessment diagram (FAD) was constructed using the fracture mechanics parameters to estimate the failure stress of the cladding. It was found from the FAD that the predicted failure stress of the cladding qualitatively agreed with the experimental results obtained by burst tests at elevated temperatures for the hydrided Zircaloy cladding tube at Japan Atomic Energy Research Institute.

Keywords: Zircaloy; Zirconium hydride; Fracture mechanics; Finite element method; Elevated temperature

1. Introduction

In recent years, the burn up of light water reactor (LWR) fuels has been increased due to prudent utilization of uranium resources and economical advantage. The failure conditions of the high burn up fuel rods under reactivity initiated accident (RIA), as well as normal operating conditions, are required for the structural integrity evaluation. In the Nuclear Safety Research Reactor (NSRR) of the Japan Atomic Energy Research Institute (JAERI), a series of experiments making use of pulse irradiation capability has been performed to study the high burn up fuel behavior during RIAs [1]. It was found from the experiments that the failure resulted from pellet-clad mechanical interaction (PCMI) accompanied by hydrogen embrittlement. In order to simulate the PCMI that occurs during the pulse irradiation in the NSRR, burst tests have been carried out at room temperature and 620 K in the JAERI [2,3]. In these tests, the fracture behavior and the burst pressure for the following types of cladding were examined:

- Type I: as received cladding without hydrogenation
- Type II: hydrided cladding with zirconium hydride accumulated locally beneath the outer surface of the cladding
- Type III: hydrided cladding with zirconium hydride distributed uniformly and with their platelet planes oriented in the circumferential direction of the cladding.

The fracture mechanism of these types of claddings has already been well analyzed by elasto-plastic finite element method (FEM) by the present authors [4]. Tables 1 and 2

Table 1
Burst pressure measured in the burst tests at room temperature [2]

Type of sample	Hydrogen concentration (wtppm)	Burst pressure (MPa)
Type I	10	123–124
Type II	520	77
Type III	166	124
	352	124
	461	126

*Corresponding author. Tel.: +81-6-6879-7905; fax: +81-6-6879-7889.
E-mail address: mkuroda@nucl.eng.osaka-u.ac.jp (M. Kuroda).

0925-8388/02/$ – see front matter
PII: S0925-8388(01)01492-X

Table 2
Burst pressure measured in the burst tests at 620 K [3]

Type of sample	Hydrogen concentration (wtppm)	Burst pressure (MPa)
Type I	10	74.5–75.0
Type II	230	73.0
Type III	504	71.4
	194	71.9
	236	72.4
	355	73.4
	387	72.4

show the test results of the burst pressure at room temperature and 620 K, respectively, at the pressurization rate of 0.002 MPa/ms (low-pressurization-rate burst test). From these tables, Type II reveals a considerably lower burst pressure than Type III with the same average hydrogen concentration at room temperature, while the burst pressure of Type II is nearly equal to that of Type III at 620 K. As for the experimental results at room temperature, the present authors have already elucidated the origin of the burst pressure degradation in terms of fracture mechanics [5]. The purpose of the present study is to interpret the test results of the burst pressure at 620 K by fracture mechanics.

In the present study, FEM analysis was performed for the models of the cladding to estimate the fracture mechanics parameters such as stress intensity factor (SIF), *J*-integral and plastic yield load. The failure assessment diagram (FAD), which was required for the estimation of the failure stress of the cladding, was constructed using the calculated fracture mechanics parameters. The experimental results of the burst test at 620 K are discussed in terms of the FAD.

2. Analytical

2.1. Modeling

The burst test apparatus in the JAERI is schematically shown in Fig. 1a. Hydraulic internal pressure was applied to Zircaloy-4 cladding tubes with inner and outer diameters of 8.36 mm and 9.50 mm, respectively, and a length of 160 mm. In the burst test, deformation in the axial direction was restricted at the lower end of the tube, while the upper end was without restriction. In the present analysis, the axial total deformation was ignored, and the plane strain condition was assumed where the axial strain is null ($\epsilon_Z = 0$), as shown in Fig. 1b. In addition, since the radial stress (σ_r) can be neglected for such a thin-walled cylinder, the burst test is assumed to be equivalent to a tension test for a panel as shown in Fig. 1c.

In the present analysis, the matrix and the zirconium hydride were considered as αZr and $\delta ZrH_{1.73}$, respectively. Since, even at 620 K, the terminal solid solubility (TSS) was much lower than the total hydrogen content at the material, all hydrogen absorbed in the αZr was assumed to precipitate the hydride completely. Where the average hydrogen concentration was 1000 mass parts per million (wtppm), the volume ratio of the $\delta ZrH_{1.73}$ to the αZr was about 5%. Types II and III modeling are illustrated in Fig. 2 where the hydrides exist only at one side of the tension panel in Type II; in Type III, 11 lines of the hydride plates are spaced equally in the axial direction of the panel.

The present authors have previously measured the mechanical properties of solid zirconium hydride by a tensile test at room temperature for a sheet-type specimen with gauge length of 5 mm, and the fracture strength of $\delta ZrH_{1.73}$ was obtained [4]. From the result of FEM analysis by the use of the experimental data of hydride, it was found that the hydride phase in the cladding tube was

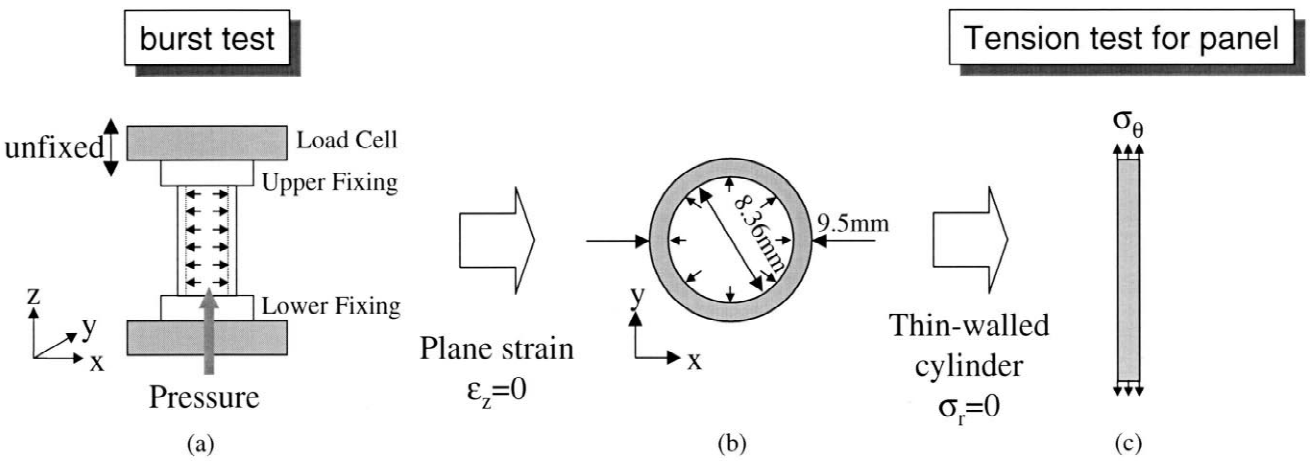

Fig. 1. Modeling of the burst test.

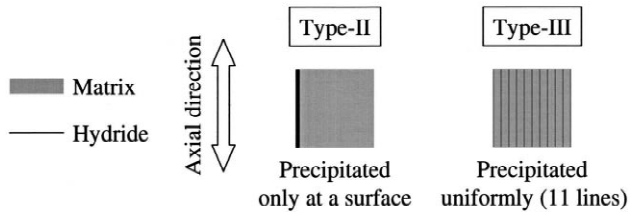

Fig. 2. Schematic illustration of the simulated distribution of hydride for panels.

fractured at much lower internal pressure than the yield point of the matrix [4]. Therefore, even at elevated temperatures, the precipitated hydrides would readily produce cracks under a low tensile loading. In the present study, it was assumed that the matrix–hydride debonding was neglected. Since river patterns within the cleavage facets were observed by scanning electron microscopy (SEM) [2], cleavage would occur at the hydride phase of the cladding. The cleavage occurs when the tensile component of the external applied stress is beyond the bond strength. Therefore, the fracture surface of the hydride plate would be oriented normal to the direction of the applied uniaxial load. Thus, the model described in Fig. 3 was employed in the present study: Types II and III have pre-existing cracks in the hydride phase. These models have the dimension of $10\times5\times1$ cm^3 and each have the same width of ligament.

2.2. Finite element method analysis

In the present study, FEM analysis was carried out to estimate fracture mechanics parameters such as SIF (K_I), J-integral (J) and plastic yield load (P_y) by the general-purpose program MARC, in which creep and dynamic effect was not considered. For Type III modeling, the SIF and J-integral were calculated at the surface and internal crack tip. The mechanical properties of αZr required for the analysis were obtained by the tensile tests at 616 K, the results of which are shown in Table 3 and Fig. 4. Only the datum of plane strain fracture toughness (K_{IC}) was substituted for Zircaloy-2 at 533 K [6] because of no experimental data for αZr.

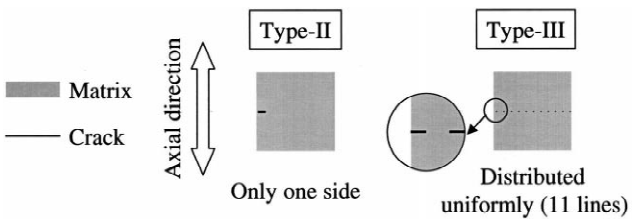

Fig. 3. Schematic illustration of the simulated distribution of cracks for panels.

Table 3
Mechanical properties used in the analysis

	E (GPa)	σ_y (MPa)	σ_u (MPa)	K_{IC} (MPa$\sqrt{m}$)
αZr	76.9	152	170	79.5

E, Young's modulus; σ_u, ultimate tensile strength; σ_y, yield stress; K_{IC}, plane strain fracture toughness.

2.3. Failure assessment diagram

In the present study, the FAD was constructed by using the estimated fracture mechanics parameters. The details of the FAD were described elsewhere [5].

3. Results and discussion

Fig. 5 illustrates the FAD at 620 K where the failure assessment curves (FACs) for the models and the cut-off line $L_r = L_r^{max} = 1.06$ are shown. As reference data, the FAD at room temperature that was formerly reported by the present authors [5] is shown in Fig. 6. Assessment points with coordinates (L_r, K_r) for these models are lined as the 'load-increasing lines'. As shown in these diagrams, both the load-increasing line of Types II and III at 620 K intersects the cut-off line, although Type II at room temperature intersects the FAC. The intersection of the load-increasing line and the cut-off line corresponds to the initiation of plastic collapse. The plastic collapse load P_C is expressed as follows [5]

$$P_C = \frac{\sigma_f}{\sigma_y} \cdot P_y \quad (1)$$

$$\sigma_f = \frac{\sigma_y + \sigma_u}{2} \quad (2)$$

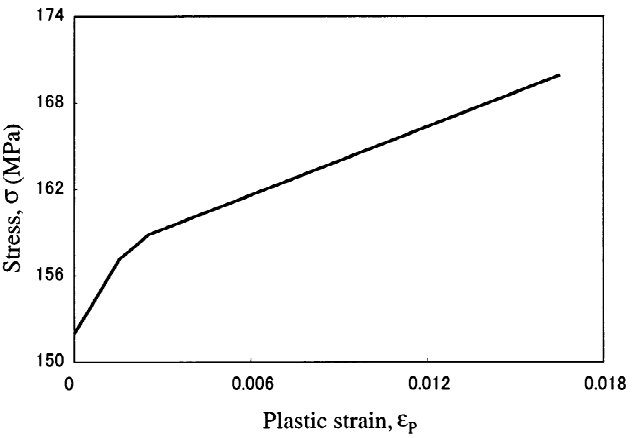

Fig. 4. Stress–plastic strain diagram of αZr at 616 K.

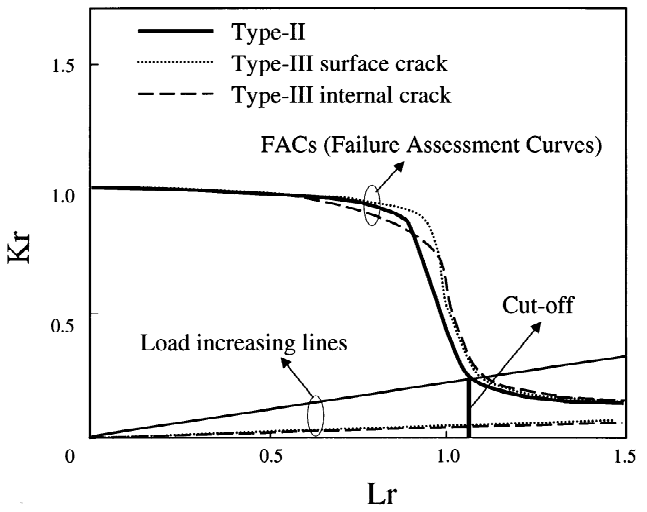

Fig. 5. FAD for the models at 620 K.

where σ_f, σ_y and σ_u are the flow stress, the yield stress and the ultimate tensile strength, respectively. Since P_y is calculated to have an approximately equal value 8.75×10^4 N for Types II and III, P_C also has the same value as those for both models. These are in good agreement with the experimental results obtained by JAERI listed in Tables 1 and 2.

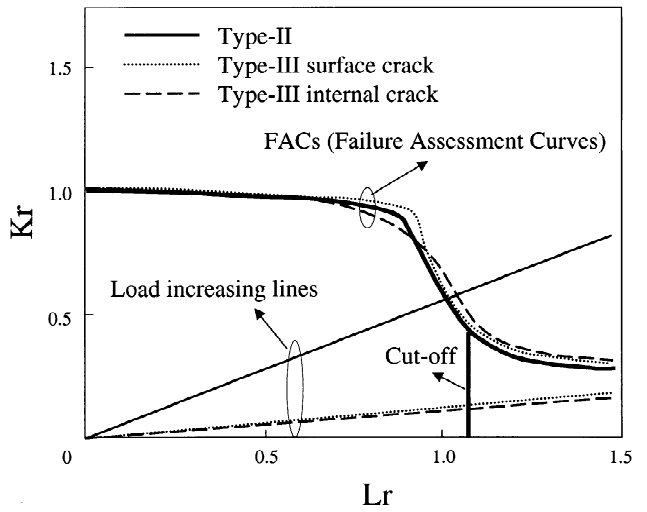

Fig. 6. FAD for the models at room temperature [5].

4. Conclusion

In the present study, an analysis based on fracture mechanics at 620 K has been carried out for several types of hydrided Zircaloy cladding tubes to elucidate the fracture behavior of high burn up LWR fuel cladding during RIAs. Fracture mechanics parameters such as SIF, *J*-integral and plastic yield load were estimated by FEM analysis using the material properties of α-phase of zirconium required for the analysis obtained by tensile tests at 616 K. The FAD was constructed using the fracture mechanics parameters to estimate the failure stress of the cladding. The FAD indicated that the failure load of the claddings with zirconium hydride accumulated locally beneath the outer surface of the cladding (Type II) was nearly equal to the claddings with zirconium hydride distributed uniformly and oriented in the circumferential direction of the cladding (Type III). These results were consistent with the experimental results obtained by burst tests at elevated temperatures for the hydrided Zircaloy cladding tube at the JAERI.

Acknowledgements

The authors would like to thank Mr. K. Moriwaki of Nippon Marc Co., for his kind instruction on the use of program system MARC. This work was supported by the Japan Atomic Energy Research Institute (JAERI).

References

[1] T. Fuketa, H. Sasajima, Y. Mori, K. Ishijima, J. Nucl. Mater. 248 (1997) 249.
[2] F. Nagase, T. Otomo, H. Uetsuka, JAERI-Research 98-064, Japan Atomic Energy Research Institute, 1998, [in Japanese].
[3] F. Nagase, T. Otomo, H. Uetsuka, JAERI-Research 2000-046, Japan Atomic Energy Research Institute, 2000, [in Japanese].
[4] M. Kuroda, K. Yoshioka, S. Yamanaka, H. Anada, F. Nagase, H. Uetsuka, J. Nucl. Sci. Technol 37 (2000) 670.
[5] M. Kuroda, S. Yamanaka, F. Nagase, H. Uetsuka, Nucl. Eng. Des. 203 (2001) 185.
[6] F.H. Huang, J. Nucl. Mater. 207 (1993) 103.